Preliminary Estimation of Engineering Bedrock Depths from Microtremor Array Measurements in Solo, Central Java, Indonesia

Sorja Koesuma,[1,5] Mohamad Ridwan,[2] Andri Dian Nugraha,[3] Sri Widiyantoro[3,4] & Yoichi Fukuda[5]

[1]Department of Physics, Sebelas Maret University, Surakarta, Indonesia
[2]Research Institute for Human Settlement (RIHS),
Ministry of Public Works and Housing, Jakarta, Indonesia
[3]Global Geophysics Group, Faculty of Mining and Petroleum Engineering,
Institut Teknologi Bandung, Jalan Ganesha 10, Bandung 40132, Indonesia
[4]Research Center for Disaster Mitigation,
Institut Teknologi Bandung, Jalan Ganesha 10, Bandung 40132, Indonesia
[5]Graduate School of Sciences, Kyoto University, Kyoto, Japan
Email: sorja@uns.ac.id

Abstract. In the last decade the city of Solo, located in Central Java, Indonesia, has grown significantly and become a major city. Many industries and hotels have been built in the city and its surroundings. This study aimed to determine the engineering bedrock depths in Solo, an important parameter in seismic hazard analysis. The microtremor array method was used to obtain 1D S-wave velocity profiles and construct layer depth maps. The spatial autocorrelation (SPAC) method was used to calculate the dispersion curves, while the S-wave velocity structure was derived using a genetic algorithm (GA). The results of the S-wave velocity structure in Solo show that there are four stratigraphic layers, where the engineering bedrock depths in Solo exist within the range from 145 to 185 m. The shape of the bedrock basin is elongated in an east-west direction.

Keywords: *engineering bedrock; genetic algorithm; microtremor; spatial autocorrelation; Solo.*

1 Introduction

Earthquakes are a natural phenomenon and they occur abruptly. It cannot be predicted when, where, or how strong they will be. Their impact is typically very significant and often causes substantial losses due to infrastructure damages and/or fatalities. The impact of an earthquake with a certain magnitude is often very diverse. Ground shaking on the surface is influenced by local geological conditions such as the hardness and thickness of the sediment overlying the engineering bedrock, which contributes to the shaking and is related to seismic wave amplification. Therefore, knowing the depth and position of the engineering bedrock is very important in seismic risk analysis.

Received May 20th, 2016, 1st Revision April 3rd, 2017, 2nd Revision August 9th, 2017, Accepted for publication August 11th, 2017.
 ISSN: 2337-5760, DOI: 10.5614/j.math.fund.sci.2017.49.3.8

Efforts to reduce the impact of earthquakes include constructing national seismic hazard maps based on the results of related studies, such as seismicity analyses (e.g. Nugraha, *et al*. [1], subsurface seismic structural imaging (e.g. Zulfakriza, *et al*. [2], identification and calculation of source parameters, and improving the procedures and the calculation of seismic hazard analysis (Irsyam, *et al*. [3]). However, seismic hazard analysis on a city scale (microzonation) must take into account the effects of local soil conditions above the engineering bedrock. In this case, it is important to identify the depth of the bedrock, which contributes to the variation in the level of earthquake damage. Typically, subsurface investigations to identify engineering bedrock are performed by drilling. However, due to the high costs involved in such studies, a microtremor array method was used instead in this study.

The microtremor method was first proposed by Aki [4] and was then developed further by Okada [5], Tada, *et al*. [6] and Nakahara [7]. Some applications of microtremor methods include the determination of the bedrock or basement depth (Motazedian, *et al*. [8], Paudyal, *et al*. [9], Stephenson, *et al*. [10], and Ridwan, *et al*. [11-13]) and site characterization (Asten, *et al*. [14], Chávez-García and Kang [15], Mohamed [16], Putra, *et al*. [17]). Additionally, the principles and practices of seismic microzonation are described in Nath [18], Sitharam [19], and Tada, *et al*. [6].

Since seismic risk analysis must be evaluated based on surface seismic hazard analysis, the sediment thickness above the engineering bedrock and its associated parameters are very important. Until now, information regarding the depth of the engineering bedrock in the study area has been unavailable. In this study, we have conducted subsurface investigations using a microtremor array method at eight observation sites in order to estimate the bedrock position and depth in the study area.

2 Geological and Seismicity Preview

The geology of the city of Solo is part of the regional geology of the Surakarta-Giritontro Quadrangle, an area covered with quaternary sediment that is mainly alluvium. The stratigraphic sequence is as follows: metamorphic rocks consisting of schist, marble, altered volcanic rocks and altered sedimentary rocks, which are the oldest rock formations in this area. The sedimentary rocks over the metamorphic rocks are tertiary sediment, i.e. Nampol formation consisting of conglomerate, sandstones, siltstone, claystone and tuff, and Oyo formation consisting of tuffaceous marl, andesitic tuff and limestone conglomerate [20].

Considering that an earthquake is still effective within a 500-km impact radius, Solo is considered a high-risk area for seismic events due to the presence of seismic activities around the city (Figure 1). Moreover, the Opak, Lasem, and Kendeng Faults are not far from Solo. Figure 1 shows the distribution of epicenter events with a magnitude of more than 5.0 on the Richter scale from January 2009 to December 2016, based on the data catalog of the Indonesian Meteorological, Climatological, and Geophysical Agency (BMKG). These events may be associated with the seismic source zone in and around Java, namely the subduction segment along the Sunda Trench and the shallow crustal faults on Java Island.

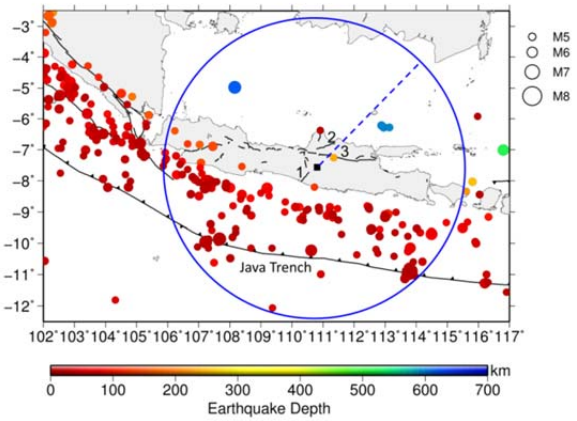

Figure 1 Epicenter distribution of earthquakes around Java from January 2009 to December 2016 with magnitudes greater than 5.0 (colored circles) in a 500 km (blue circle) radius from Solo (black square), based on the BMKG data catalog. The three main faults located around the study area are indicated by numbers 1 (Opak), 2 (Lasem), and 3 (Kendeng).

3 Method

3.1 Data Aquisition

Microtremor measurements were performed at eight locations throughout the city of Solo and its surroundings; the distance between observation sites was approximately 3 km (Figure 2). The field survey for deep layers at each observation site used an equilateral triangular shape with a size of 400 m, 200 m and 100 m, assuming bedrock depths of less than 400 m. Four units of microtremor data recorders were deployed at each triangular array; one unit was placed in the center of the triangle and the others were placed at every corner of the triangle (Figure 3). Simultaneous recordings of microtremor data were conducted on each triangular array in a two-hour time duration. The

microtremor recording unit (MRU) used in the field survey is a type of seismograph with high magnification and consists of a portable vertical component sensor with a characteristic frequency band of 0.1-200 Hz and a 32-bit analog to digital converter (ADC). A sampling interval of 0.01 sec was used for data recording. Each seismometer was equipped with a GPS navigation system used for synchronization in order for all recordings to occurr simultaneously.

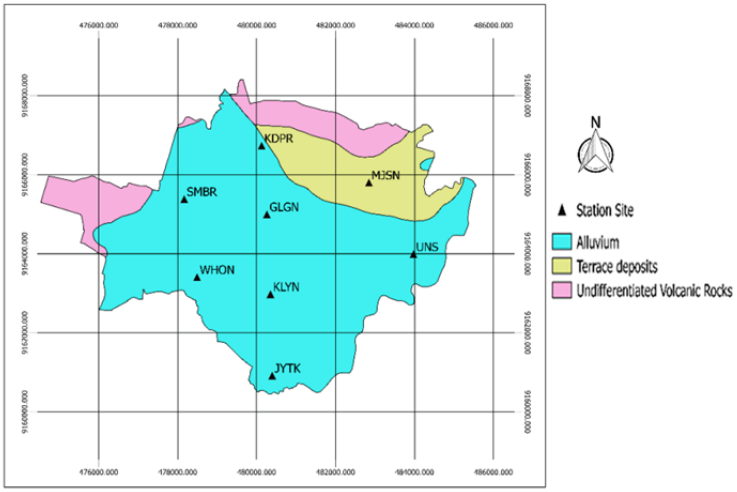

Figure 2 Map with the microtremor survey sites in the Solo area depicted by black triangles. Different colors stand for rock types in the study area as shown in the legend (modified from Surono, *et al*. [20]). The letters next to each triangle are station codes.

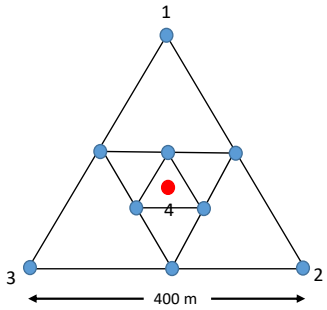

Figure 3 Equilateral triangle configuration employed in this study. Simultaneous recording of microtremor data was carried out using four seismometers that were placed in the center and at the edges of the triangle. The size of the triangle determines the depth of the detected layers.

3.2 Spatial Autocorrelation (SPAC) Method

Since microtremor waves are defined as Rayleigh waves, the vertical component data were processed. The time series of recorded microtremors was digitized using a sampling interval of 0.01 sec and divided into time windows of 163 sec. By using a triangular array configuration, it was possible to calculate the phase velocity by applying the spatial autocorrelation (SPAC) method (Aki [4], Okada [5], and Morikawa [21]). The SPAC function can be derived for a pair of stations in a circular array. The coefficient of SPAC was then calculated by averaging all the azimuths to obtain the phase velocity at each frequency (dispersion curves). Since the dispersion curve is a function of the subsurface structure, it can be used to estimate the S-wave velocity structure by using an inversion technique.

3.3 Inversion of Dispersion Curves

Following Yamanaka and Ishida [22], a genetic algorithm (GA) was applied for the inversion of the dispersion curves using a specified initial model. The inversion process was generated on a search area with a population of 20 individuals, determined randomly. The individuals were selected by minimizing a misfit function (see [22] for further details).

Table 1 Search limits of S-wave velocity and thickness.

Layer No.	Vs range (m/sec)	Depth range (m)	Density (g/cm^3)
1	317 - 477	24 - 36	1.8
2	417 - 627	60 - 90	1.9
3	494 - 742	108 - 162	1.9
4	576 - 866	168 - 252	2.0
5	611 - 917	240 - 360	2.0

The GA was generated in the specified search area to the dispersion curves of the fundamental modes of Rayleigh waves using GA parameters as in Yamanaka and Ishida [22]: crossover probability at 0.7 and mutation probability at 0.02. The population number was determined randomly and then generated for 20 iterations to obtain a minimum misfit. This inversion was conducted by assuming that the layer models were horizontal, isotropic, homogenous, and consisted of two parameters to be estimated, i.e. S-wave velocity and thickness, while density was fixed for each layer. The search limits of the S-wave velocity and thickness are shown in Table 1. The assumed density of each layer is also shown in the same table.

4 Results and Discussion

4.1 Dispersion Curves

The dispersion curve of microtemors at each observation site was calculated using the SPAC method (Figure 4). In general, the frequency of the dispersion curves ranged from 1.2 to 6.0 Hz, while the phase velocity, which is mostly influenced by local geological conditions, ranged from 200 to 800 m/sec. These curves reflect the variation of the subsurface conditions at each observation site, namely the thickness and hardness used to estimate the 1D S-wave velocity profile using the genetic algorithm.

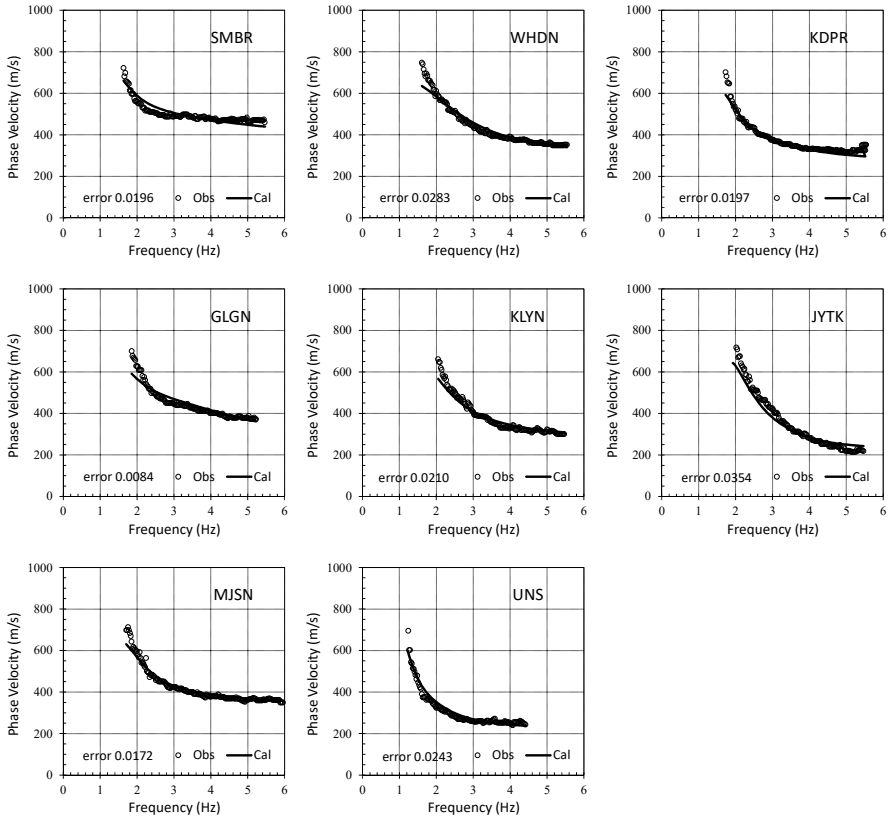

Figure 4 Fitting of calculated and observed dispersion curves for each measurement site.

4.2 1D S-Wave Velocity (Vs) Profiles from the First Inversion

Estimation of the S-wave velocity structure was carried out using a genetic algorithm, which is an optimization method with guided random search. A

search with GA was performed using an initial model to obtain the smallest misfit between the dispersion based on calculation and observation. By referring to the geological conditions around Solo, the initial model was determined to have five layers representing rock formations [20]. The GA was employed to the dispersion curves using this initial model. The results from all observation sites are shown in Figure 5; they are 1D S-wave velocity profiles showing the layer depths.

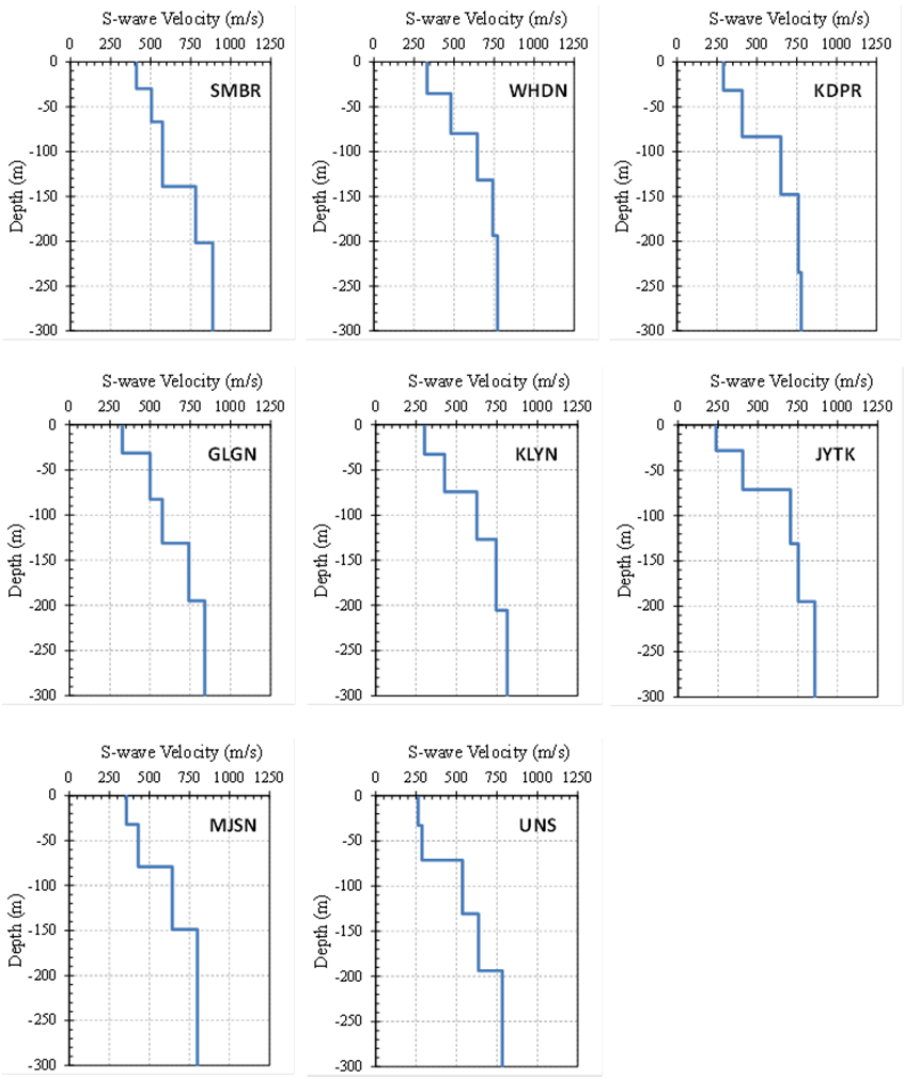

Figure 5 1D S-wave velocity profiles resulting from the first inversion at all sites.

Table 2 and Figure 6 show the estimated engineering bedrock depths at each site in Solo. The deepest part reaching 208 m is located in the southern part of the study area, i.e. beneath station KLYN.

Table 2 Depths of engineering bedrock for Vs > 750 m/sec.

No	Station (code)	Long (deg)	Lat (deg)	Engineering Bedrock	
				Vs (m/sec)	Depth (m)
1	Sumber (SMBR)	110.803	– 7.550	782	139
2	Wahidin (WHDN)	110.806	– 7.568	771	193
3	Kadipiro (KDPR)	110.821	– 7.538	778	148
4	Gilingan (GLGN)	110.822	– 7.554	839	195
5	Kemlayan (KLYN)	110.823	– 7.572	814	208
6	Joyotakan (JYTK)	110.823	– 7.591	753	195
7	Mojosongo (MJSN)	110.846	– 7.546	800	149
8	UNS (UNS)	110.856	– 7.563	783	194

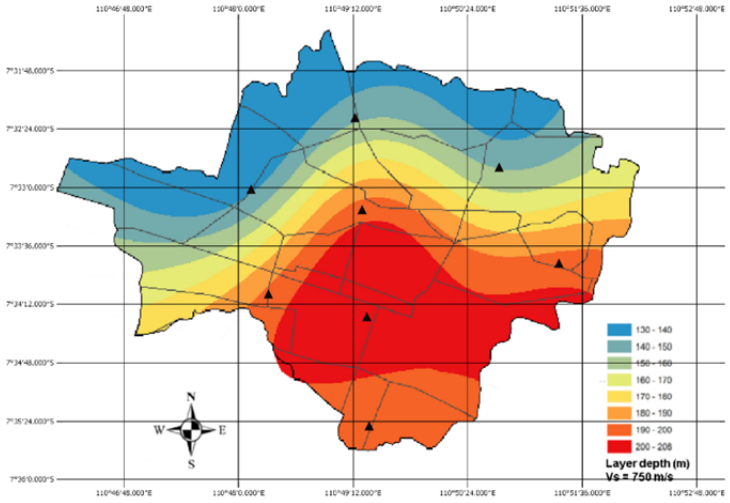

Figure 6 Map of layer depths for Vs > 750 m/sec. Black triangles and blue lines depict survey sites and city roads, respectively.

4.3 1D S-Wave Velocity Structures from the Second Inversion

Construction of the velocity (Vs) structure was performed using correlations of the same velocity for each layer as derived from the 1D Vs profiles resulting from the first inversion (Figure 5). The depths of the layers with the same velocity were obtained by performing the second inversion with the average Vs in each layer. This technique was proposed by Yamanaka and Yamada [23] for reconstructing the depth of bedrock in the Kanto Basin, Japan.

The 1D Vs profiles depict the model as consisting of five layers with a velocity ranging from 250 to 850 m/sec. According to the National Standardization Agency (BSN [24]), the engineering bedrock layer is the layer with Vs > 750 m/sec, which can be determined from the first inversion results. In the SMBR, WHDN, KDPR, and MJSN locations, the engineering bedrock is in the fourth layer, while in GLGN, KLYN, JYTK, and UNS it is in the fifth layer. The depths of the layers with the same velocity were obtained by making a sketch in order to obtain the initial model for the second inversion.

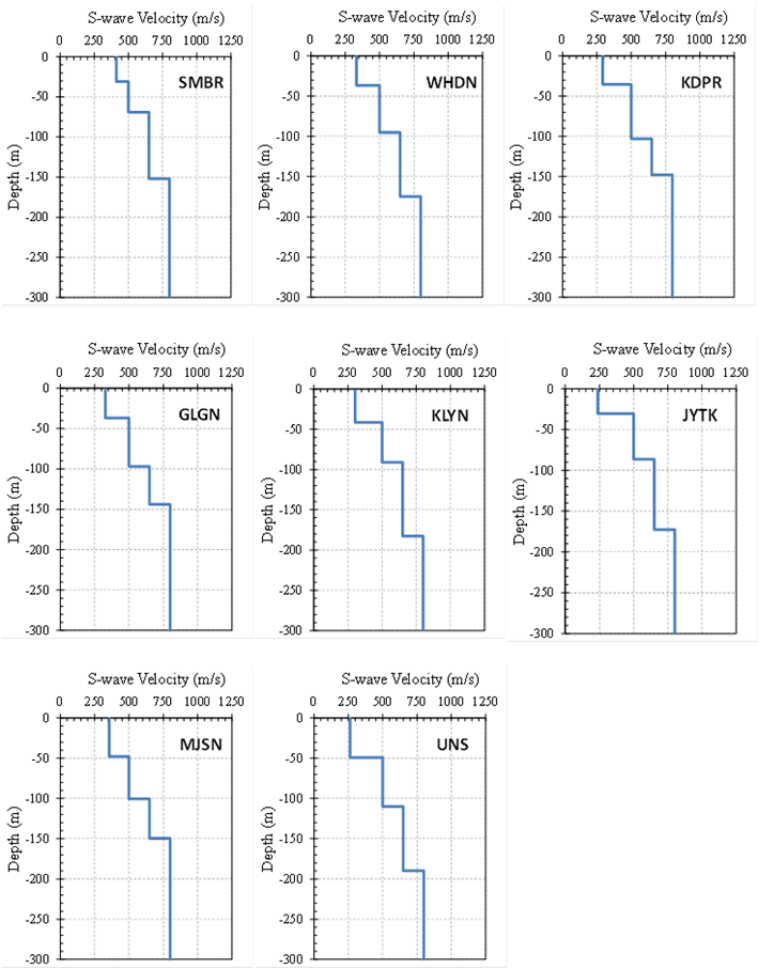

Figure 7 The same as Figure 5, but obtained from the second inversion.

Judging from the 1D profiles as a whole, the reconstruction of the initial model for the second inversion was done for four layers, with the second to the fourth layers having velocities of 500, 650 and 800 m/sec, respectively; the first layer

velocity is determined according to the original Vs because it is close to the actual condition. This model was inverted again towards the dispersion curves for each site in order to obtain new layer depths. The second inversion results show 1D profiles with the same velocity in the second to the fourth layers (Figure 7), allowing the spatial correlation process. The distribution of layer depths was spatially constructed from the second inversion results; the depths of the layers are shown in Figures 8-10. Figures 8 and 9 show the maps of layer depths for Vs = 500 m/sec and Vs = 650 m/sec, respectively. Figure 10 depicts the map of the layer depths for Vs = 800 m/sec, which is identified as engineering bedrock depths, which vary from 145 to 185 m.

The deepest part of the engineering bedrock roughly extends in an east-west direction. Meanwhile, the bedrock is quite shallow in the northern part of the study area, having a depth of around 145 m. It reaches deeper southward; in the center of the Solo area, the depth reaches 200 m. However, the bedrock becomes shallow again in the southernmost part of the study area with depths of about 170-175 m. The east-west trend of the deepest engineering bedrock is in agreement with the results of the first inversion of 1D profiles in which Vs > 750 m/sec (Figure 6).

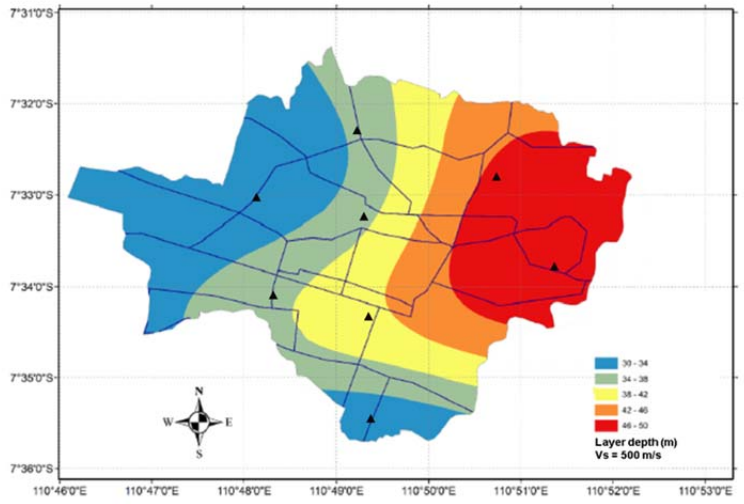

Figure 8 Map of layer depths for Vs = 500 m/sec based on the results of the second inversion. Black triangles and blue lines depict survey sites and city roads, respectively.

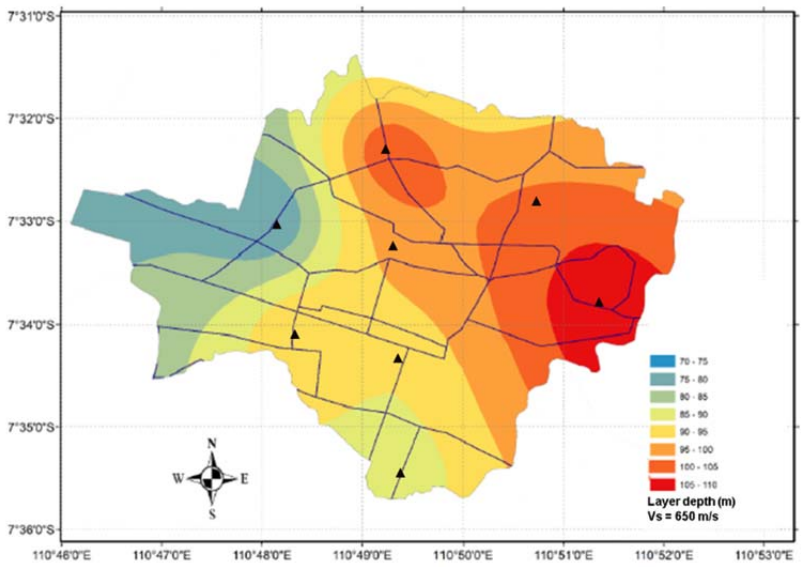

Figure 9 Same as Figure 8, for Vs = 650 m/sec.

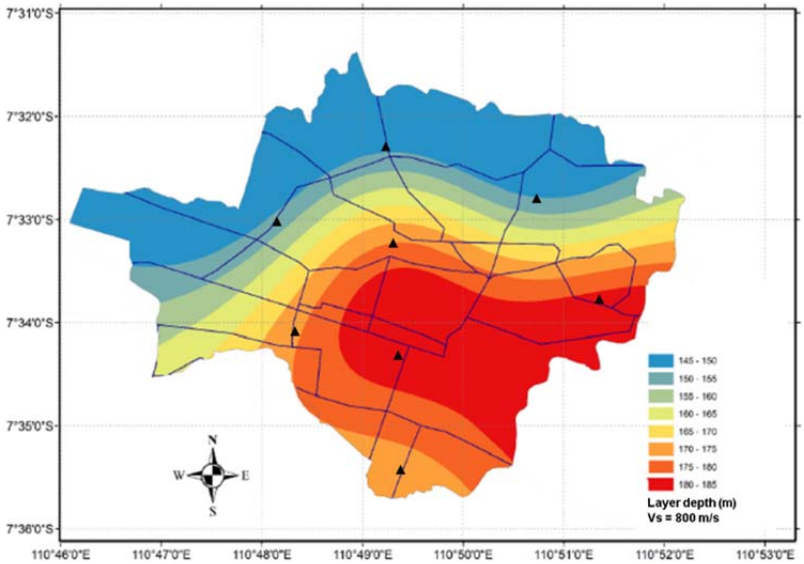

Figure 10 Same as Figure 8, for Vs = 800 m/sec.

A summary of the layer depths beneath all stations for Vs = 500, 650 and 800 m/sec is given in Table 3.

Table 3 Layer depths for Vs = 500, 650 and 800 m/sec.

No	Station (code)	Layer depths (m)		
		Vs = 500 m/sec	Vs = 650 m/sec	Vs = 800 m/sec
1	Sumber (SMBR)	31	69	152
2	Wahidin (WHDN)	36	95	175
3	Kadipiro (KDPR)	35	102	148
4	Gilingan (GLGN)	37	97	144
5	Kemlayan (KLYN)	41	91	183
6	Joyotakan (JYTK)	31	87	173
7	Mojosongo (MJSN)	48	101	150
8	UNS (UNS)	49	110	190

5 Conclusions

The results of microtremor array surveys at eight sites in the Solo area show that the 1D S-wave velocity profiles resulting from the first inversion consist of five layers of varying depths (Figure 5). In the top layer, S-wave velocities ranging from 237 to 412 m/sec, associated with the distribution of sediment hardness, were obtained. The estimated engineering bedrock was located in the fifth layer (130-208 m depth) with Vs > 750 m/sec. The deepest engineering bedrock (depth > 200 m) was found to the south of the central part of the city, extending in an east-west direction. The depth of the engineering bedrock becomes shallower and reaches about 130-140 m in the northernmost part of the city.

From the results of the second inversion, a four-layer model was obtained. The top of the second layer with Vs = 500 m/sec has depths ranging from 30 to 50 m, and the top of the third layer with Vs = 650 m/sec has depths ranging from 50 to 110 m, while the top of the fourth layer with Vs = 800 m/sec varies in depth from 110 to 190 m. Based on these Vs values, the engineering bedrock for the city of Solo is located in the fourth layer. In general, it was shown that the form of the Solo bedrock basin is elongated and orientated in an east-west direction.

The S-wave velocity profiles resulting from the first and second inversions are comparable. However, the results of the second inversions are more preferable because the construction of the Vs profiles was performed using correlations of the same velocity for each layer, thereby making them easier to interpret. The deepest engineering bedrock depths are located in the alluvium region as shown in the geological model of Solo (Figure 2). This spatial distribution of layer depths is important for surface seismic hazard analysis. The deep engineering

bedrock depths imply that the associated part of the city of Solo (indicated by a red color in Figure 10) will have higher seismic wave amplification due to the thicker sediment.

In the future, we plan to conduct microtremor array measurements using more stations in Solo and its surrounding areas. By doing this, we hope to delineate the basin structure beneath the study region in greater detail.

Acknowledgments

The authors gratefully acknowledge the Research Institute for Human Settlement (RIHS), the Ministry of Public Works and Housing of the Republic of Indonesia, and the Indonesian Association of Geophysicists (HAGI) for their support of the fieldwork needed to acquire the data used in this study. Thanks also go to the Indonesian Meteorological, Climatological, and Geophysical Agency for access to their data catalog.

References

[1] Nugraha, A.D., Shiddiqi, H.A., Widiyantoro, S., Sutiyono & Handayani, T., *Analysis of Spatiotemporal Variation in b-Value for the Sunda Arc Using High Precision Earthquake Location*, AIP Conference Proceedings, 1730, art. no. 020003, 2016. DOI: 10.1063/1.4947371.

[2] Zulfakriza, Z., Saygin, E., Cummins, P.R., Widiyantoro, S., Nugraha, A. D., Lühr, B-G. & Bodin, T., *Upper Crustal Structure of Central Java, Indonesia, from Transdimensional Seismic Ambient Noise Tomography*, Geophysical Journal International, **197**(1), pp. 630-635, 2014. DOI: 10.1093/gji/ggu016.

[3] Irsyam, M., Sengara, I. W., Asrurifak, M., Ridwan, M., Aldiamar, F., Widiyantoro, S., Triyoso, W., Natawijaya, D. H., Kertapati, E., Meilano, I. & Suhardjono, *Development of Seismic Hazard Maps of Indonesia for Revision of Seismic Hazard Map in SNI 03-1726-2002*, Research Report Submitted to the Ministry of Public Works by Team for Revision of Seismic Hazard Maps of Indonesia, 2010. (Text in Indonesian)

[4] Aki, K., *Space and Time Spectra of Stationary Stochastic Waves, with Special Reference to Microtremors,* Bulletin of the Earthquake Research Institute, 1957.

[5] Okada, H., *Theory of Efficient Array Observations of Microtremors with special reference to the SPAC Method,* Exploration Geophysics, **37**(1), pp. 73-85, 2006. DOI:10.1071/EG06073

[6] Tada, T., Cho, I. & Shinozaki, Y., *Beyond the SPAC Method: Exploiting the Wealth of Circular-Array Methods for Microtremor Exploration,*

Bulletin of the Seismological Society of America, **97**(6), pp. 2080-2095, 2007. DOI:10.1785/0120070058

[7] Nakahara, H., *Formulation of the Spatial Autocorrelation (SPAC) Method in Dissipative Media,* Geophysical Journal International, **190**(3), pp. 1777-1783, 2012. DOI:10.1111/j.1365-246X.2012.05591.x

[8] Motazedian, D., Hunter, J.A., Pugin, A. & Crow, H., *Development of a Vs 30 (NEHRP) Map for the City of Ottawa, Ontario, Canada*, Canadian Geotechnical Journal, **48**(3), pp. 458-472, 2011. DOI:10.1139/T10-081

[9] Paudyal, Y.R., Yatabe, R., Bhandary, N.P. & Dahal, R.K., *Basement Topography of the Kathmandu Basin using Microtremor Observation*, Journal of Asian Earth Sciences, **62**, pp. 627-637, 2013. DOI:10.1016/ j.jseaes.2012.11.011

[10] Stephenson, W.J., Hartzell, S., Frankel, A.D., Asten, M., Carver, D.L. & Kim, W.Y., *Site Characterization for Urban Seismic Hazards in Lower Manhattan, New York City, from Microtremor Array Analysis*, Geophysical Research Letters, **36**(3), pp. 1-5, 2009. DOI:10.1029/ 2008GL036444

[11] Ridwan, M., Afnimar, Widiyantoro, S., Irsyam, M. & Yamanaka, H., *Estimation of S-Wave Velocity Structures by Using Microtremor Array Measurements for Subsurface Modeling in Jakarta*, J. Math. Fund. Sci., **46**(3), pp. 313-327, 2014. DOI:10.5614/j.math.fund.sci.2014.46.3.9

[12] Ridwan, M., Widiyantoro, S., Afnimar & Irsyam, M., *Identification of Engineering Bedrock in Jakarta by Using Array Observations of Microtremors,* Procedia Earth and Planetary Science, **12**, pp. 77-83, 2015.

[13] Ridwan, M., Widiyantoro, S., Irsyam, M., Afnimar & Yamanaka, H., *Development of Engineering Bedrock Map beneath Jakarta Based on Microtremor Array Measurements*, Geological Society, London, **441**(1), pp.153-165, 2016.

[14] Asten, M.W., Askan, A., Ekincioglu, E. E., Sisman, F.N. & Ugurhan, B., *Site Characterisation in North-Western Turkey based on SPAC and HVSR Analysis of Microtremor Noise*, Exploration Geophysics, **45**(2), pp. 74-85, 2014. DOI:10.1071/ EG12026

[15] Chávez-García, F.J. & Kang, T.S., *Lateral Heterogeneities and Microtremors: Limitations of HVSR and SPAC Based Studies for Site Response*, Engineering Geology, **174**, pp. 1-10, 2014. DOI:10.1016/ j.enggeo.2014.02.007

[16] Mohamed, A., *Site Characterization and Seismic Site Response Study of the Sahary Area*, South Egypt, Acta Geodynamica et Geomaterialia, **12**(4), pp. 1-10, 2015. DOI:10.13168/ AGG.2015.0032

[17] Putra, R.R., Kiyono, J., Yoshimoto, Y. & Ono, Y., *Determined Soil Characteristic of Palu in Indonesia by Using Microtremor Observation*, Int. J. of GEOMATE, **10**(2), pp. 1737-1742, 2016.

[18] Nath, S.K., *Seismic Microzonation Framework – Principles & Applications*, Proceedings of Workshop on Microzonation, pp. 9-35, 2007.
[19] Sitharam, T.G., *Seismic Microzonation: Principles, Practices and Experiments*, Electronic Journal of Geotechnical Engineering, Bouquet 08, pp. 1-58, 2008.
[20] Surono, Toha, B. & Sudarno, I., *Geological Map - Giritontro Surakarta*, Java, Scale 1:100,000, Geological Research and Development Center, Bandung, Indonesia, 1992. (Text in Indonesian).
[21] Morikawa, H., *A Method to Estimate Phase Velocities of Rayleigh Waves Using Microseisms Simultaneously Observed at Two Sites*, Bulletin of the Seismological Society of America, **94**(3), pp. 961-976, 2004. DOI:10.1785/0120030020
[22] Yamanaka, H. & Ishida, H., *Application of Genetic Algorithms to an Inversion of Surface-Wave Dispersion Data*, Bulletin of the Seismological Society of America, **86**(2), pp. 436-444, 1996.
[23] Yamanaka, H. & Yamada, N., *Estimation of 3D S-Wave Velocity Model of the Kanto Basin, Japan, Using Rayleigh Wave Phase Velocity*, Bulletin of the Earthquake Research Institute, **81**(3/4), pp. 295-301, 2006.
[24] BSN, *Planning Procedures for Earthquake Resistance for a Review of Building and Non-Buildingstructures*, National Standardization Agency of Indonesia, 2012. (Text in Indonesian)